

LETTER TO THE EDITOR

GG Tau: the fifth element^{*}

E. Di Folco^{1,2}, A. Dutrey^{1,2}, J.-B. Le Bouquin³, S. Lacour⁴, J.-P. Berger⁵, R. Köhler⁶, S. Guilloteau^{1,2}, V. Piétu⁷,
J. Bary⁸, T. Beck⁹, H. Beust³, E. Pantin¹⁰

¹ Univ. Bordeaux, Laboratoire d'Astrophysique de Bordeaux, UMR 5804, F-33270, Floirac, France

² CNRS, LAB, UMR 5804, F-33270 Floirac, France

e-mail: emmanuel.difolco@obs.u-bordeaux1.fr

³ UJF-Grenoble 1/CNRS-INSU, Institut de Planétologie et d'Astrophysique de Grenoble UMR 5274, F-38041, Grenoble, France

⁴ LESIA, CNRS/UMR-8109, Observatoire de Paris, UPMC, Université Paris Diderot, 5 place J. Janssen, F-92195, Meudon, France

⁵ European Southern Observatory, D-85748, Garching by München, Germany

⁶ Max-Planck-Institut für Astronomie, Königstuhl 17, D-69117 Heidelberg, Germany

⁷ IRAM, 300 rue de la piscine, F-38406 Saint-Martin d'Hères, France

⁸ Department of Physics and Astronomy, Colgate University, 13 Oak Drive, Hamilton, NY 13346, USA

⁹ Space Telescope Science Institute, 3700 San Martin Dr. Baltimore, MD 21218, USA; tbeck@stsci.edu, lubow@stsci.edu

¹⁰ Laboratoire AIM, CEA/DSM - CNRS - Université Paris Diderot, IRFU/SAP, F-91191, Gif-sur-Yvette, France,

Received 19 February 2014, Accepted 10 March 2014

ABSTRACT

We aim at unveiling the observational imprint of physical mechanisms that govern planetary formation in young, multiple systems. In particular, we investigate the impact of tidal truncation on the inner circumstellar disks. We observed the emblematic system GG Tau at high-angular resolution: a hierarchical quadruple system composed of low-mass T Tauri binary stars surrounded by a well-studied, massive circumbinary disk in Keplerian rotation. We used the near-IR 4-telescope combiner PIONIER on the VLTI and sparse-aperture-masking techniques on VLT/NaCo to probe this proto-planetary system at sub-au scales. We report the discovery of a significant closure-phase signal in H and K_s bands that can be reproduced with an additional low-mass companion orbiting GG Tau Ab, at a (projected) separation $\rho = 31.7 \pm 0.2$ mas (4.4 au) and $PA = 219.6 \pm 0.3^\circ$. This finding offers a simple explanation for several key questions in this system, including the missing-stellar-mass problem and the asymmetry of continuum emission from the inner dust disks observed at millimeter wavelengths. Composed of now five co-eval stars with $0.02 \leq M_\star \leq 0.7 M_\odot$, the quintuple system GG Tau has become an ideal test case to constrain stellar evolution models at young ages (few 10^6 yr).

Key words. Stars: binaries: close - Planetary systems: proto-planetary disks - Techniques: high angular resolution, interferometry

1. Introduction

Planet formation is a common process that can occur in different environments. While the first decade of planet searches has preferentially focused on single, solar-like host stars, it has been more recently shown that a large proportion of extrasolar giant planets are born in binary systems (Udry & Santos 2007). The recent discoveries of transiting circumbinary planets in close binary systems (Kepler 16, 34, 35, Doyle et al. 2011; Welsh et al. 2012), as well as the planet candidate directly imaged around the young low-mass binary 2MASS J0103 (Delorme et al. 2013) have proven that planets can also appear in a circumbinary disk, despite the strong dynamical mechanisms that shape the disk and can rapidly clear out its inner region. Stars in young binary systems are expected to be surrounded by two inner disks, located inside the Roche lobes and an outer circumbinary ring or disk outside the outer Lindblad resonances (e.g., Artymowicz & Lubow 1994). Persistent signs of accretion in binary systems, as well as direct imaging of residual gas in the inner region, demonstrate that gas and dust can flow from the outer reservoir through this gravitationally unstable zone to nurture inner circumstellar disks (where planet formation may also occur), which otherwise would not survive. Understanding how the inner disks are re-

plenished is also important in the general context of planetary system formation, since binary stars provide a scaled-up version of a proto-planet environment in a circumstellar (CS) disk. Finally, multiple systems can provide essential clues in testing stellar evolution models, as they provide a set of co-eval stars with different masses at a common distance (e.g., White et al. 1999)

In the past two decades, the young hierarchical quadruple system GG Tau, composed of two low-mass binary systems, has been subject of many detailed studies. With its relatively massive ($0.15 M_\odot$) and bright outer ring, GG Tau A is one of the best known nearby (140 pc) T Tauri binaries, with a $0.26''$ separation (36 au on the sky plane). The circumbinary disk ($R_{in} = 180$ au) has been observed in thermal dust emission (Dutrey et al. 1994; Guilloteau et al. 1999; Piétu et al. 2011) and in scattered light (Roddier et al. 1996; Silber et al. 2000), and is in Keplerian rotation (Dutrey et al. 1994). The scattered-light images proved that the gravitationally unstable zone is not empty of dust. Indirect evidence for gas flow from the ring towards the inner system(s) has been found from ^{12}CO J=2-1 gas image (Guilloteau & Dutrey 2001) and from near-IR H_2 transitions (Beck et al. 2012). The warm H_2 gas may be heated by shocks, as material from the circumbinary ring is accreted onto material close to the stars. The existence of inner CS disks is independently attested by mm excess emission on GG Tau Aa (Piétu et al. 2011), strong

^{*} Based on ESO programs 090.C-0339(A,F)

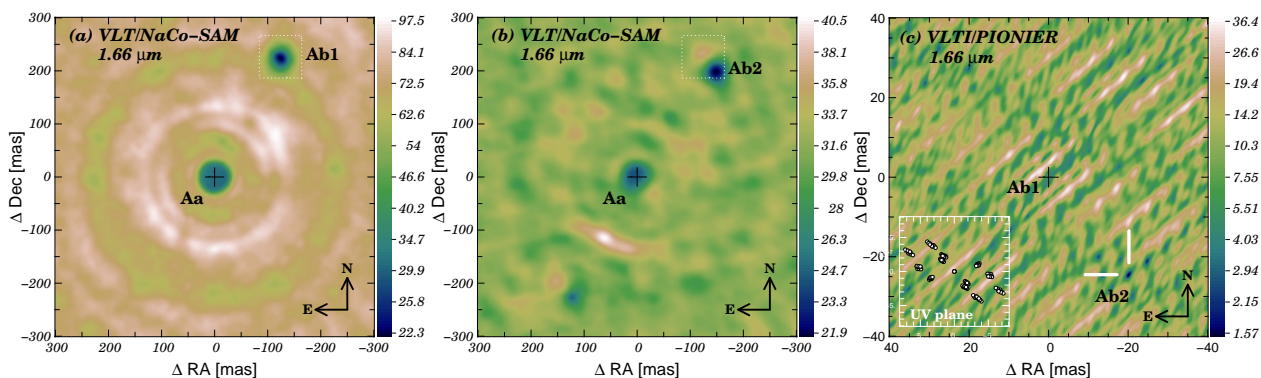


Fig. 1. Chi2 maps for: NACO-SAM H -band closure-phase data (6+7 Dec. 2012): location of GG Tau Ab1 (a) and Ab2 (b) around the primary star GG Tau Aa, and for PIONIER (c) H -band closure-phase data for Ab2 location around Ab1, with VLTI (u, v) sampling in the inset.

H_α accretion signature separately detected around Aa and Ab, [OI] line detection around Ab (White et al. 1999; Hartigan & Kenyon 2003), and $10\mu\text{m}$ silicate feature from hot grains in both Aa and Ab environments (Skemer et al. 2011). We have recently undertaken a very high-spatial resolution observing program of GG Tau A, from UV to mm wavelengths. In this letter, we report near-IR VLT interferometric observations of the inner region of the GG Tau A system, where we detect a new component and direct evidence for resolved circumstellar dust emission.

2. Observations and data analysis

We observed the GG Tau A system on 2012 October 30 with the VLTI, using the four 8 m Unit Telescopes (UTs) on baseline lengths between 32 and 140 m, and the PIONIER instrument (Le Bouquin et al. 2011) operating in the H band ($1.5\text{--}1.8\mu\text{m}$, three spectral channels). Thanks to the combination of the MACAO adaptive optics system and the tiny interferometric field of view (FOV) of VLTI /UTs ($FWHM \sim 41$ mas in H band), we were able to separately point at the $0.26''$ binary GG Tau Aa (M0V) and Ab (M2V) with PIONIER. Seeing conditions were stable, with optical seeing values $\theta_0 \sim 0.6\text{--}0.9''$, and a coherence time in the range $\tau_0 \sim 3\text{--}5$ ms. We performed interleaved observations of two calibrator sources of known diameter (HD28462, K1V, $\Theta_{UD}^H = 0.169 \pm 0.012$ mas, and HD285720, K4V, $\Theta_{UD}^H = 0.148 \pm 0.011$ mas). Four independent series of calibrated observations were acquired, with interferometric fringes simultaneously recorded on six baselines, and reduced with the *pndrs* package (Le Bouquin et al. 2011).

We also observed GG Tau A on 2012 December 6 and 7 with the diffraction-limited imager VLT/NAOS-CONICA (Lenzen et al. 2003). We performed sparse-aperture-masking (SAM) observations on NaCo with a 7-hole mask (Tuthill et al. 2000). The mask at the pupil-plane blocks most of the light from the centered target and resamples the primary mirror into a set of smaller subapertures that form a sparse interferometric array with 21 baselines. The $0.26''$ close binary Aa–Ab is resolved in the NaCo field of view, but not by the individual subpupils. Measurements of closure-phases (CP) allow one to detect high-contrast companions and proved to be more efficient than classical AO-imaging within $\sim 20\text{--}300$ mas at H and K_s -bands (Lacour et al. 2011). We used a 27 mas/pixel plate scale and high-cadence frame acquisition mode, the science target itself being used for the IR wavefront sensing. On Dec. 6, data were recorded with the H and K_s bands ($2.0\text{--}2.1\mu\text{m}$) filters, while H and L' filters were used on Dec. 7. Atmospheric conditions were stable ($\theta_0 \sim 0.5\text{--}0.8''$, $\tau_0 \sim 3\text{--}6$ ms). The same two calibrator sources

as for PIONIER were selected, with a fast-switch pointing sequence. The observations were reduced using the Paris SAMP pipeline as described in Lacour et al. (2011).

3. Results

The PIONIER measurement for GG Tau Aa is consistent with a marginally resolved, symmetric emission, as attested by the fringe visibility (V^2) and CP functions displayed in Fig. 2. Around the dimmer GG Tau Ab, we report the detection of a CP signal as large as 30 deg, which reveals an asymmetric brightness distribution. We attribute this feature to a third companion (Ab2) in the main binary system GG Tau A. Square visibilities also show oscillation-like structures, but we chose to rely on the CP values to derive the binary characteristics, because they are less affected by atmospheric phase fluctuations and known telescope vibrations. We used the LITPRO software¹ (Tallon-Bosc et al. 2008) to extract the Ab1–Ab2 binary flux ratio and astrometric position by independently fitting the PIONIER and NaCo-SAM data (Table 1). A simple model with two unresolved stars yields a good fit to the CP values ($\chi_{\text{red}}^2 = 1.5$ vs 7.1 for a single star), with a raw flux ratio of 8.1 ± 2.1 (H -band). We derive a separation of 31.7 ± 0.2 mas and a position angle $PA = 219.6 \pm 0.3$ deg (Fig. 1).² Because the IR photo-center of Ab1–Ab2 is closer to Ab1 and their separation represents about 30% of the instrumental FOV (i.e., an 8 m telescope Airy disk), we applied a correction for the FOV attenuation. The correction factor (based on a Gaussian-profile attenuation of $FWHM = 41$ mas, centered on the K_s -band centroid) amounts to $f_{\text{corr}} = 0.53$. (The uncertainty on f_{corr} depends on the AO and tip-tilt stabilizer performance; we evaluate $\delta f_{\text{corr}} \sim 0.2$ for a residual uncertainty 4 mas rms on the position of the Ab1–Ab2 centroid). The attenuation-corrected PIONIER flux ratio for a two-point source-model becomes $(F_{\text{Ab1}}/F_{\text{Ab2}})_{\text{corr}} = 4.3 \pm 1.1 \pm 1.6$ (the second term is due to δf_{corr} only), that is $\Delta H \sim 1\text{--}2$ mag.

The two components of GG Tau A were simultaneously observed with NaCo. The CP values are dominated by the Aa–Ab binary, and we first fit its position: the 256 mas separation is consistent with long-term astrometric studies (Köhler 2011), and the flux ratios agree with literature data. We then added a third component Ab2 by fitting its location relative to Aa and its flux ratio. The Ab1–Ab2 close binary is well constrained by the

¹ www.jmmc/litpro

² Because of the limited (u, v) coverage with VLTI, a second position for Ab2 is possible ($\rho = 32.5 \pm 0.2$ mas, $PA = 230.0 \pm 0.4$ deg), although less likely ($\chi_r^2 = 2.0$).

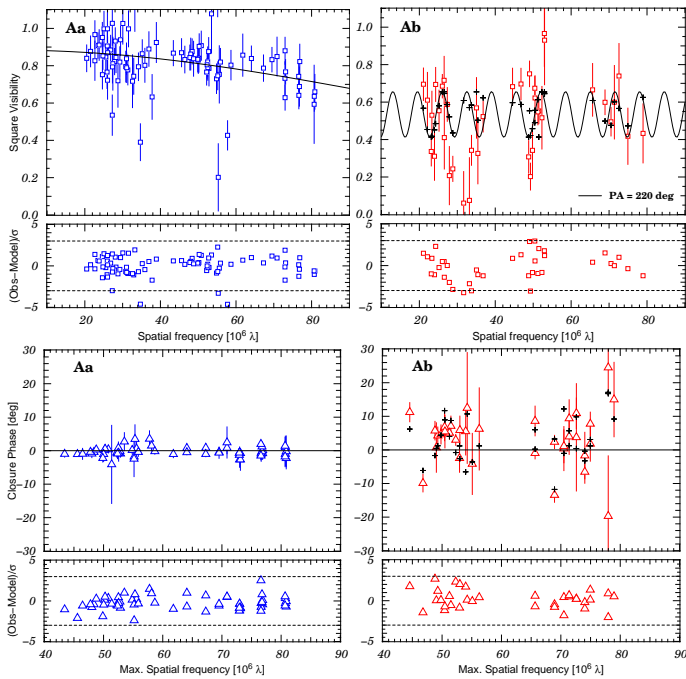


Fig. 2. VLT/PIONIER square visibilities (squares, top panels) and closure phases (triangles, bottom panels) separately measured for GG Tau Aa (left, blue) and Ab1+2 (right). Solid lines or cross markers represent best-fit models: unresolved photosphere, halo and ring for Aa (model-2 in Table 3), and 2 unresolved photospheres and a halo for Ab (model-4). Below each plot we display the fit residuals.

NaCo data, and the three-component model always yields a better fit. The best-fit positions are consistent with each other at H and K_s bands, as well as with the VLTI estimate (although with larger uncertainties, see Table 1). We adopted an averaged separation of 31.6 ± 3.3 mas and $PA = 222.6 \pm 6.0$ deg with NaCo. In the less angularly resolved L' band, we fixed the binary separation to its mean value and only fit the flux ratio (2.6 ± 0.4). The mask subaperture sizes correspond to an equivalent pupil diameter of 1.2 m, hence a 350 mas point spread function (PSF) in H band. To properly account for the resulting flux attenuation, we oversampled the Fourier plane by a factor of 3. The derived NaCo-SAM flux ratios are then 1.6 ± 0.4 and 2.4 ± 0.3 at H and K_s bands, respectively. These values were used to estimate the spectral type of Ab2. Surprisingly, the inferred Ab1/Ab2 H -band flux ratio appears to be lower than our PIONIER estimate (4.3 ± 2.3). This discrepancy is discussed in Appendix A.

4. Discussion

4.1. Nature of the detected component

A non zero closure-phase indicates a non axisymmetric brightness distribution, which may either be interpreted as the presence of a stellar companion, or as a brightness asymmetry in the disk emission. Similar detections with SAM techniques have recently been reported for a few other young sources with known protoplanetary disks (e.g., T Cha, Huélamo et al. 2011). For these transitional disks, it has been demonstrated that starlight scattered off the inner edge of the outer disk (typically at $R \sim 10$ au) can equally well reproduce the detected closure-phase as a (sub)stellar companion (Ölofsson et al. 2013; Cieza et al. 2013). However, the CP amplitudes in these systems are much smaller than for GG Tau Ab (≤ 1 deg, implying much higher IR contrasts $\Delta mag \sim 5$). It also requires the disk to have a high inclination (at

least 60 deg) for forward-scattering by μm -sized grains to be efficient at the gap outer edge. We judge a disk-origin to be highly unlikely, since we detect a CP as large as 30 deg.

We calculated the probability P for the CP to be caused by contamination from a background source. P is evaluated from the surface density $\rho(m)$ of sources brighter than $m = H + \Delta H = 9.1 + 2.5 = 11.6$ (worst case) around GG Tau A: $P(\Theta, m) = 1 - \exp^{-\pi \rho(m) \Theta^2}$ (Brandner et al. 2000). With 591 sources within a $\Theta \leq 1$ deg radius circle around GG Tau A (after 2MASS, Cutri et al. (2003)), P is only 10^{-7} at a maximum separation of $0.032''$.

Finally, re-examining archival NaCo data from December 2003 brings another argument in favor of a companion. We employed a procedure similar to that described in Köhler et al. (2000): we extracted subframes around GG Tau Aa and Ab and applied speckle-interferometric techniques to compute the modulus of the visibility of Ab, using Aa as a PSF reference. The visibility shows clear signs of a close companion. A binary model was fitted, resulting in an Ab1–Ab2 separation of 28 ± 3 mas, $PA = 65 \pm 5$ deg [mod 180 deg], and a flux ratio of 4.6 ± 1.0 (K_s -band). This *a posteriori* detection further supports the bound-companion hypothesis. Assuming a circular orbit in the sky plane, we derive a crude estimate of the orbital period $P = 16 \pm 1$ yr for clockwise (CW) rotation from the 9 yr separated positions. Interestingly, this result agrees well with the orbital period derived according to the spectral type and stellar mass estimates (see Sect. 4.2 below), and CW rotation was also independently derived for the outer disk (from the CO velocity field, Guilloteau et al. 1999) and for the Aa–Ab orbit.

4.2. Characteristics of the new triple stellar system

If we assume that the close binary orbit is coplanar with the outer disk, the de-projected separation of Ab1 and Ab2 was 5.1 au in Dec. 2012. Following the spectroscopic analysis of Hartigan & Kenyon (2003), the bright system GG Tau A is composed of Aa, an M0 star ($\sim 0.6 M_\odot$), and of Ab, which displays a M2V spectral type ($\sim 0.38 M_\odot$ for a single star). Hartigan & Kenyon (2003) noted that the inferred spectral type for Ab leads to an insufficient stellar mass in the system in comparison with the dynamical mass estimate of $1.28 \pm 0.07 M_\odot$ (for a distance of 140 pc) derived from the CO gas kinematics in the ring by Guilloteau et al. (1999). We assume here that this spectral type M2 can be attributed to the brighter component Ab1.

If we assume that the relative flux excesses around Ab1 and Ab2 are roughly similar, the reported contrast approximates the stars contrast. Combining all flux ratio constraints in H , K_s and L' bands (see Table 1), and using the spectral type-color relations (Bessell et al. 1991; Leggett 1992), we propose that Ab2 is an M3 ± 0.5 dwarf star, with a mass $0.25 - 0.35 M_\odot$ (Hartigan & Kenyon 2003) leading to a binary mass ratio $q_{Ab1-Ab2} = 0.8 \pm 0.2$. If the orbit of Ab1–Ab2 is circular and coplanar with the outer ring, with a total stellar (dynamical) mass of $0.58 - 0.75 M_\odot$ and a semi-major axis of 5.1 ± 0.4 au, its orbital period is estimated to $P = 14^{+3}_{-2}$ yr from Kepler laws. If the relative IR flux excess were much higher around Ab1 than Ab2, it would bias the spectral type estimate for Ab2 towards earlier types (i.e., $q \sim 1$).

We note that a slightly better solution to the PIONIER CP fit might be found with a third component in the GG Tau Ab system, that is, if Ab2 were itself a close binary. Such models are degenerated: several solutions exist with Ab2a–Ab2b separations of 10–15 mas ($1.5 - 2.3$ au, i.e., about a third of the distance between Ab1 and the Ab2 barycenter), yielding $\chi^2_{red} \sim 1$ instead of 1.5 ($dof = 27$), with a flux ratio $F_{Ab2a}/F_{Ab2b} \sim 1.5 - 3$. A sig-

	PIONIER		NACO-SAM		NACO-SAM		NACO-SAM		NACO-SAM	
	H (2012-10-30)		H (2012-12-06/07)		K_s (2012-12-06)		$H + K_s$		L' (2012-12-07)	
	best-fit	σ	best-fit	σ	best-fit	σ	mean	σ	best-fit	σ
ρ [mas] Aa - Ab			256.1	1.5	255.8	3.5	256.1	1.3	256.3	3.3
PA [deg] Aa - Ab			329.6	0.3	329.3	0.8	329.5	0.4	328.9	0.8
F(Aa) / F(Ab)			2.36	0.04	1.99	0.04			1.88	0.23
ρ [mas] Ab1 - Ab2	31.7	0.2	31.7	4.1	31.6	5.8	31.6	3.3	31.4	fixed
PA [deg] Ab1 - Ab2	219.6	0.3	219.9	7.3	227.6	10.3	222.6	6.0	219.9	fixed
F(Ab1) / F(Ab2)	4.3 ^(*)	2.3 ^(*)	1.6	$^{+0.6}_{-0.2}$	2.3	0.2			2.8	0.2

Table 1. Relative astrometric position and flux contrast for the main binary Aa-Ab (photo-center of Ab1-Ab2), and for the close binary Ab1-Ab2, as derived from our best-fit of the closure phases measured by VLT/NaCo-SAM and VLTI/PIONIER. The formal errors on NaCo-SAM PA do not include uncertainties due the detector orientation. (*): after correction for FOV attenuation (see text), the related uncertainty dominates

nificantly improved (u, v) coverage would be necessary to decide for one of the two scenarios.

Finally, the analysis of the PIONIER visibilities, in combination with an independent estimate of the excess flux around Aa and Ab from literature photometry, allows one to partly constrain the presence and characteristics of circumstellar material in the two systems. The related discussion can be found in Appendix A, where we show that Aa may be surrounded by a CS disk revealed by its marginally resolved bright inner rim, while the dust distribution around Ab1 and Ab2 might be more complicated.

4.3. Consequences for the dynamics of the system

In addition to solving the missing-stellar-mass problem, the discovery of a fifth component in this system provides a logical explanation for the lack of submm/mm continuum emission around Ab attested by PdBI (Piétu et al. 2011) and ALMA observations (Dutrey et al. 2014, submitted). The Ab1 and Ab2 components are indeed surrounded by Roche lobes of radius ~ 2 au. Tidal truncation effects naturally prevent the existence of stable disk(s) larger than this limit, and thus not massive enough to be strong mm emitters, in contrast to Aa. The $10\mu\text{m}$ silicate emission probably arises from warm grains located within 2 au (i.e., well inside the Roche lobes). The resulting gravitational disturbance may also affect the supply of material from the outer regions through dust and gas streamers, as it breaks the symmetry of the Aa-Ab system. The close binary GG Tau Ab also strengthens the impact of tidal truncation onto the circumbinary ring. However, the location of its inner rim (180 au), which is much more distant than the apparent separation of the Aa and Ab(1+2) components, remains a puzzling characteristics of the system.

5. Conclusion

The emblematic, young binary system GG Tau A ($0.26''$ separation) has been successfully observed with interferometric and AO/sparse-aperture-masking techniques (SAM) at the Very Large Telescope. We found that:

1. The secondary GG Tau Ab is itself a close binary, with a projected separation of $0.032''$ (or 4.5 au) and $PA = 220^\circ$ (end 2012). It is consistent with a M3V (Ab2) and M2V (Ab1) low-mass binary. This finding solves the discrepancy between the dynamical stellar mass derived from CO gas kinematics (Guilloteau et al. 1999) and the most recent spectral-type estimate of Aa and Ab (Hartigan & Kenyon 2003). Based on a tentative *a posteriori* identification in archival (2003) VLT/NACO images, its orbital period is estimated to

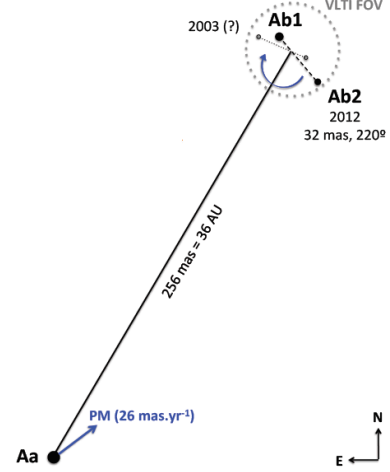


Fig. 3. Sketch of the new triple system GG Tau Aa (M0V), Ab1 (M2V), and Ab2 (M3V) in their 2012 orbital configuration.

$P_{\text{Ab1-Ab2}} \sim 16$ yr, a value consistent with the period derived from the binary mass and separation.

2. All stars in this triple system present significant IR excesses, confirming the presence of circumstellar material. Around GG Tau Aa, the NIR emission is partly resolved at $1.65\mu\text{m}$ and the derived geometrical ring radius is typical of protoplanetary disks around low-luminosity stars. For GG Tau Ab, due to tidal truncation, a (deprojected) separation of ~ 5.1 au sets a strong constraint on the maximum radial extent of any circumstellar disk surrounding Ab1 and/or Ab2 ($R_{\text{out}} \lesssim 2$ au). The binary nature of this system also provides a simple explanation to the intriguing non detection of mm continuum emission at the location of Ab.
3. With five coeval low-mass stars, this young multiple system becomes an ideal test case to constrain evolutionary models, provided that future astrometric studies will refine the stars physical parameters of the Ab system.

Acknowledgements. We acknowledge the "Programme National de Physique Stellaire" and the "Programme National de Planétologie" (CNRS/INSU, France) for financial support. This research has made use of the Jean-Marie Mariotti Center SearchCal and LITpro services co-developed by FIZEAU and IPAG.

References

- Akeson, R. L., Walker, C. H., Wood, K., et al. 2005, *ApJ*, 622, 440
 Artymowicz, P. & Lubow, S. H. 1994, *ApJ*, 421, 651
 Bate, M. R. & Bonnell, I. A. 1997, *MNRAS*, 285, 33
 Beck, T. L., Bary, J. S., Dutrey, A., et al. 2012, *ApJ*, 754, 72
 Bessell, M. S., Brett, J. M., Scholz, M., & Wood, P. R. 1991, *A&AS*, 89, 335

- Brandner, W., Zinnecker, H., Alcalá, J. M., et al. 2000, *AJ*, 120, 950
- Cieza, L. A., Lacour, S., Schreiber, M. R., et al. 2013, *ApJ*, 762, L12
- Cutri, R. M., Skrutskie, M. F., van Dyk, S., et al. 2003, 2MASS All Sky Catalog of point sources.
- Delorme, P., Gagné, J., Girard, J. H., et al. 2013, *A&A*, 553, L5
- Doyle, L. R., Carter, J. A., Fabrycky, D. C., et al. 2011, *Science*, 333, 1602
- Dutrey, A., Di Folco, E., Guilloteau, S., et al. 2014, *Nature*, submitted
- Dutrey, A., Guilloteau, S., & Simon, M. 1994, *A&A*, 286, 149
- Guilloteau, S. & Dutrey, A. 2001, in *IAU Symposium*, Vol. 200, The Formation of Binary Stars, ed. H. Zinnecker & R. Mathieu, 229
- Guilloteau, S., Dutrey, A., & Simon, M. 1999, *A&A*, 348, 570
- Hartigan, P. & Kenyon, S. J. 2003, *ApJ*, 583, 334
- Huélamo, N., Lacour, S., Tuthill, P., et al. 2011, *A&A*, 528, L7
- Köhler, R. 2011, *A&A*, 530, A126
- Köhler, R., Kasper, M., & Herbst, T. 2000, in *IAU Symposium*, Vol. 200, IAU Symposium, 63P
- Lacour, S., Tuthill, P., Amico, P., et al. 2011, *A&A*, 532, A72
- Le Bouquin, J.-B., Berger, J.-P., Lazareff, B., et al. 2011, *A&A*, 535, A67
- Leggett, S. K. 1992, *ApJS*, 82, 351
- Lenzen, R., Hartung, M., Brandner, W., et al. 2003, in *Society of Photo-Optical Instrumentation Engineers (SPIE) Conference Series*, Vol. 4841, Society of Photo-Optical Instrumentation Engineers (SPIE) Conference Series, ed. M. Iye & A. F. M. Moorwood, 944–952
- Mathis, J. S. 1990, *ARA&A*, 28, 37
- Monnier, J. D., Berger, J.-P., Millan-Gabet, R., et al. 2006, *ApJ*, 647, 444
- Olofsson, J., Benisty, M., Le Bouquin, J.-B., et al. 2013, *A&A*, 552, A4
- Piétu, V., Gueth, F., Hily-Blant, P., Schuster, K.-F., & Pety, J. 2011, *A&A*, 528, A81
- Pinte, C., Ménard, F., Berger, J. P., Benisty, M., & Malbet, F. 2008, *ApJ*, 673, L63
- Roddier, C., Roddier, F., Northcott, M. J., Graves, J. E., & Jim, K. 1996, *ApJ*, 463, 326
- Silber, J., Gledhill, T., Duchêne, G., & Ménard, F. 2000, *ApJ*, 536, L89
- Skemer, A. J., Close, L. M., Greene, T. P., et al. 2011, *ApJ*, 740, 43
- Tallon-Bosc, I., Tallon, M., Thiébaud, E., et al. 2008, in *Society of Photo-Optical Instrumentation Engineers (SPIE) Conference Series*, Vol. 7013, Society of Photo-Optical Instrumentation Engineers (SPIE) Conference Series
- Tuthill, P. G., Monnier, J. D., & Danchi, W. C. 2000, in *Society of Photo-Optical Instrumentation Engineers (SPIE) Conference Series*, Vol. 4006, Society of Photo-Optical Instrumentation Engineers (SPIE) Conference Series, ed. P. Léna & A. Quirrenbach, 491–498
- Udry, S. & Santos, N. C. 2007, *ARA&A*, 45, 397
- Welsh, W. F., Orosz, J. A., Carter, J. A., et al. 2012, *Nature*, 481, 475
- White, R. J., Ghez, A. M., Reid, I. N., & Schultz, G. 1999, *ApJ*, 520, 811

Appendix A: Inner disks constraints

Characterizing the inner circumstellar (CS) disk(s) is more challenging, because of the limited resolution of the interferometer. Not all system characteristics can be directly fitted. Using our spectral-type estimates for Aa and Ab1+2 and the resolved photometric values from the literature for Aa and Ab, we derived the relative contributions of the photospheres and of the CS material (IR excess), and use these inputs to model the VLTI data.

We first assumed that all the emission in the I band is purely photospheric in origin and we adopted an optical extinction ratio $R_V = 5$ (extinction laws from Mathis 1990), and a common reddening value A_V for Ab1 and Ab2 of 0.3 from Hartigan & Kenyon (2003). In the H band, we derive a fractional excess emission $F_d/F_{\text{tot}} = 0.32 \pm 0.16$ for Aa, and $F_d/F_{\text{tot}} = 0.61 \pm 0.12$ for Ab1+Ab2 (insensitive to the spectral type adopted for Ab2, see Table 2).

We then fit the PIONIER data with analytical models that consists of one (or two) star(s) plus a geometrically thin, circular ring to mimic the bright inner rim of the CS disk(s). For GG Tau Aa, a fully resolved component may contribute up to 7 % of the emission ($V^2 < 1$ at short baselines, see Fig. 2). Such extended components (or "halos") are common around young stars, and can reach ~ 20 % of the total emission (e.g., Akeson et al. 2005). It has been proposed that scattered light (at the disk surface or by a residual envelope) might explain this visibility drop (e.g., Monnier et al. 2006; Pinte et al. 2008). Fixing the total excess flux ratio to 32 % (model-2 in Table 3), we infer a ring radius in the range 0.05 – 0.1 au, a value consistent with the expected grain sublimation distance for a disk around a $0.38 L_\odot$ star (Pinte et al. 2008). Our observation of Aa is thus consistent with an unresolved photosphere accounting for 68 % of the H -band emission, surrounded by a canonical circumprimary disk whose inner rim bright edge remains marginally resolved by the VLTI. This disk is also known to be large and massive enough to produce detectable mm emission (Piétu et al. 2011).

In the 32 mas binary Ab, the presence of at least one CS disk is indirectly attested by the detection of the $10 \mu\text{m}$ silicate feature (Skemer et al. 2011) and classical accretion tracers (White et al. 1999). PIONIER visibilities do not show a clear drop at long baselines (Fig. 2), although the data are more noisy than for the brighter Aa. This indicates that any disk-like emission remains mostly unresolved. A fit of PIONIER data ($CP+V^2$) with two point sources and a halo-like component (see Table 3, model-4) yields $F_{\text{halo}} \sim 20$ %, $F_{\text{Ab1}} \sim 70$ % (star+ unresolved dust emission), $F_{\text{Ab2}} \sim 10$ %, and $F_{\text{Ab1}}/F_{\text{Ab2}} = 4.3 \pm 2.0$. The discrepancy with the observed NaCo contrast (1.6 ± 0.4) is hard to explain. We cannot exclude that it has an instrumental origin: the modest Strehl ratio ~ 30 % of the VLTI adaptive optics and tip-tilt correction residuals make the FOV correction delicate. However, if this discrepancy is real, it might be linked to the spatial extent and location of the halo emission in Ab. We propose that the halo might be located around Ab2, with a spatial extent in the range 10–30 mas radius (i.e., 1.5–4.5 au). It would thus be fully resolved on VLTI baselines, but would remain unresolved for NaCo, and would thus only contribute to the NaCo-SAM closure phase. This halo emission could partly originate from the complex geometry of streamers in the gravitationally unstable zone around the close binary. This is suggested by the detection of an extended warm H_2 emission around Ab, which most likely traces accretion shocks of inflowing material towards the CS disk(s) (Beck et al. 2012). If the halo and Ab2 emissions were co-located, the VLTI contrast (after correction for FOV-attenuation) would thus become $F_{\text{Ab1}}/(F_{\text{Ab2}} + F_{\text{halo}}) = 1.4 \pm 0.6$ (model-4),

in better agreement with the NaCo-SAM value. Finally, from the photometry constraints (literature data, see Table 2), we estimate that the H -band dust excess amounts to 60 ± 10 % of the total emission in Ab. Because Ab2 (star+disk) can only account for ~ 10 % of the total flux, most of the remaining 40 % excess flux should arise from the Ab1 CS environment (disk?). Theoretical simulations of binary system formation (e.g., Bate & Bonnell 1997) suggest that the primary star usually accretes more material than the secondary, and in some cases the circumsecondary disk may not even be present. Although the limited spatial information and data quality do not allow us to fully constrain the CS environments in the Ab close binary, the current data set seems consistent with this scenario.

	A_V	I		J		H		K_s		L'	
		mag	σ	mag	σ	mag	σ	mag	σ	mag	σ
Aa (obs)	0.30	10.46	0.02	9.24	0.21	8.27	0.25	7.73	0.16	6.72	0.13
Aa (dereddened)		10.26		9.14		8.21		7.69		6.81	
Aa (M0V)		10.26		9.26		8.63		8.46		8.32	
$F_{\text{excess}} / F_{\text{tot}}$		0		0.10	0.17	0.32	0.16	0.51	0.07	0.75	0.03
Ab1+Ab2 (obs)	0.45	12.19	0.04	10.12	0.21	9.07	0.32	8.53	0.24	7.69	0.04
Ab1+Ab2 (dered.)		11.89		9.97		8.98		8.47		7.66	
Ab1 (M2V)		12.16		11.01		10.31		10.11		9.95	
Ab2 (M3.5V)		13.53		12.13		11.48		11.23		11.02	
$F_{\text{Ab1}}^* / F_{\text{Ab2}}^*$ (M2/M3)		2.1		1.9		1.9		1.8		1.7	
$F_{\text{Ab1}}^* / F_{\text{Ab2}}^*$ (M2/M3.5)		3.5		2.8		2.9		2.8		2.7	
$F_{\text{excess}} / F_{\text{tot}}$ (M2/M3)		0		0.48	0.10	0.61	0.12	0.70	0.07	0.83	0.02

Table 2. Photometry of the triple system: observed apparent magnitudes from Hartigan & Kenyon (2003) for Aa and (Ab1+Ab2), extinction-corrected magnitudes, expected magnitudes from color-indices and the spectral-type estimate, expected flux ratios between stellar components for the closest spectral types, and estimated flux excess from circumstellar material for the adopted M2/M3V spectral types.

<i>GG Tau Aa - Models</i>	χ_{red}^2	$F_{\text{halo}}/F_{\text{tot}}$	$F_{\text{Ab1}}/F_{\text{tot}}$	$F_{\text{ring}}/F_{\text{tot}}$	$F_{\text{excess}}/F_{\text{tot}}$	$\Theta(\text{ring})[\text{mas}]$	R(ring) [au]
1- Point source+halo	1.4	0.10 ± 0.01	0.90 ± 0.08	–	≥ 0.11	–	–
2- Point source+halo+ring ^a	1.2	0.06 ± 0.01	0.68 (fixed)	0.26 ± 0.08	0.32 (fixed)	1.0 ± 0.2	0.07 ± 0.01
<i>GG Tau Ab1+Ab2 - Models</i>	χ_{red}^2	$F_{\text{halo}}/F_{\text{tot}}$	$F_{\text{Ab1}}/F_{\text{tot}}$	$F_{\text{Ab2}}/F_{\text{tot}}$	$F_{\text{excess}}/F_{\text{tot}}$	$(F_{\text{Ab1}}/F_{\text{Ab2}})_{\text{corr}}$	
3- 2-point sources ^b	1.5	–	0.89 ± 0.15	0.11 ± 0.02	–	4.3 ± 2.0	
4- 2-point sources+halo	2.2	0.19 ± 0.03	0.73 ± 0.09	0.08 ± 0.01	≥ 0.19	4.6 ± 1.8	

Table 3. Summary of geometrical model fits to the VLTI-PIONIER data on 2012-10-30 for GG Tau Aa and Ab(1+2) respectively. (^a): a circular ring and an elongated ring (with an aspect ratio, an inclination and orientation forced to the known circumbinary ring values) yield similar results. (^b): fit to closure-phase values alone, a single-star model would yield $\chi_{\text{red}}^2 = 7$.